



# Holographic waveguide HUD with in-line pupil expansion and 2D FOV expansion

COLTON M. BIGLER,<sup>1,\*</sup> MICAH S. MANN,<sup>1</sup> AND PIERRE-ALEXANDRE BLANCHE<sup>1,2</sup>

<sup>1</sup>James C. Wyant College of Optical Sciences, University of Arizona, 1630 E University Boulevard, Tucson, Arizona 85719, USA

<sup>2</sup>e-mail: pablanche@optics.arizona.edu

\*Corresponding author: colton.bigler@gmail.com

Received 26 July 2019; revised 14 October 2019; accepted 15 October 2019; posted 16 October 2019 (Doc. ID 373853); published 13 November 2019

**A method of head-up display is presented that uses an in-line surface relief grating attached to a waveguide propagation head-up display to achieve a large field of view without the need for large-projection optics. Horizontal pupil expansion is achieved using an extraction hologram that is multiple times the size of the injection hologram and is recorded with modulated diffraction efficiency. Vertical pupil expansion is achieved by coupling the surface relief grating to the waveguide surface between the injection and extraction holograms. The grating replicates the beam along the propagation direction, which allows for a larger field of view at the extraction. Using this technique, both a Zemax OpticStudio computer model and a physical system demonstrator achieve a field of view of  $16^\circ \times 14.25^\circ$ . © 2019 Optical Society of America**

<https://doi.org/10.1364/AO.58.00G326>

## 1. INTRODUCTION

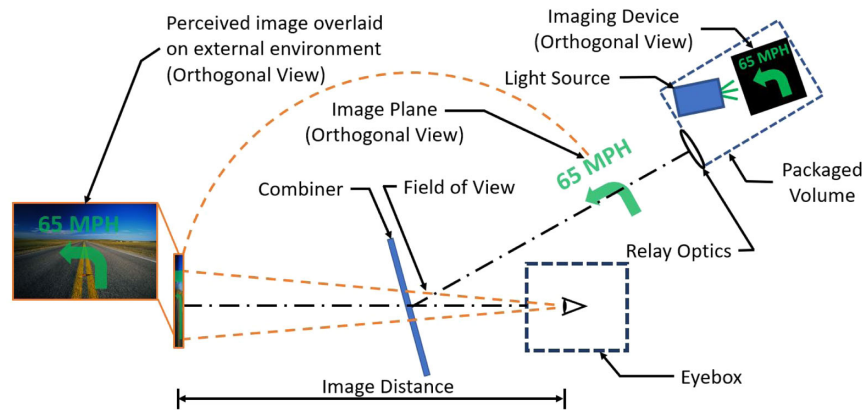
Head-up display (HUD) is a technology that shows instrument readings for operation of a vehicle in such a way that the readings can be seen without operators taking their focus away from the surrounding environment. The information is typically projected onto a windshield or visor, where it is overlaid onto the vehicle's surroundings. This means that a vehicle using an HUD system can display relevant safety, status, and control information, so that these data are visible as the user looks at the vehicle's operating environment. Displaying information in this way offers a number of advantages over traditional head-down displays (HDDs), including shorter eye accommodation times and increased eyes-forward time, both of which translate to enhanced situational awareness and faster reaction time by users [1–5].

Figure 1 shows the traditional HUD layout, where an image is projected through a collection of optics to a transparent, partially reflective combiner. From the combiner, the image is reflected back to the vehicle operator, where it appears that the image is located at optical infinity and overlaid on the external scene [6–13]. In this way, relevant control information is presented to the vehicle's operator at the same viewing distance and in the same space as the vehicle's surroundings.

Despite the advantages that HUD offers to vehicle operators, it has yet to be widely implemented in automotive applications. This is due, in part, to the limitations of the traditional projection system, chief among which is the small field of view (FOV) of the projected image [14–16]. In traditional projection

geometry, the size of the relay optics needs to be increased to project a larger image. Unfortunately, increasing the size of the relay optics, and thus the packaged volume, quickly becomes unfeasible for many vehicular applications, where space is at a premium. Additionally, the traditional projection system suffers from a small eyebox, which is the area within which the observer can move his/her head and still observe an unvignetted image.

Researchers have begun to explore the use of diffractive optics and holographic optical elements (HOEs) applied to planar waveguides as a means to achieve image magnification and pupil expansion for HUDs [17–23]. In these systems, incident light is coupled into a waveguide and diffracted beyond the critical angle by an HOE. This diffracted light propagates along the length of the waveguide due to total internal reflection (TIR) until it interacts with other HOEs, which modify the beam profile or diffract it to another propagation direction. In a previous research effort, two-dimensional (2D) pupil expansion was demonstrated using an “L-shaped” hologram configuration [23]. Figure 2 shows this L-shaped design: light from a source image is diffracted to propagate down the length of the planar waveguide by an “injection” HOE. Light incident upon the “redirection” HOE is partially diffracted by the hologram. Diffracted light is steered laterally along the length of the waveguide, while undiffracted light continues to propagate down the length of the waveguide, where it again interacts with the “redirection” hologram. Upon this subsequent interaction, another copy of the beam is steered laterally along the length of the waveguide. This expanded vertical pupil means that a larger



**Fig. 1.** In a traditional HUD, light from the source is encoded with the desired image before it passes through a collection of relay optics that cause the image to be located at optical infinity. The light is then projected onto a partially reflective, transparent combiner so that the image is reflected to the observer while still allowing him/her to see outside the vehicle. An orthogonal view of the imaging device, the image plane, and the perceived image are shown to demonstrate how an image propagates through the system.

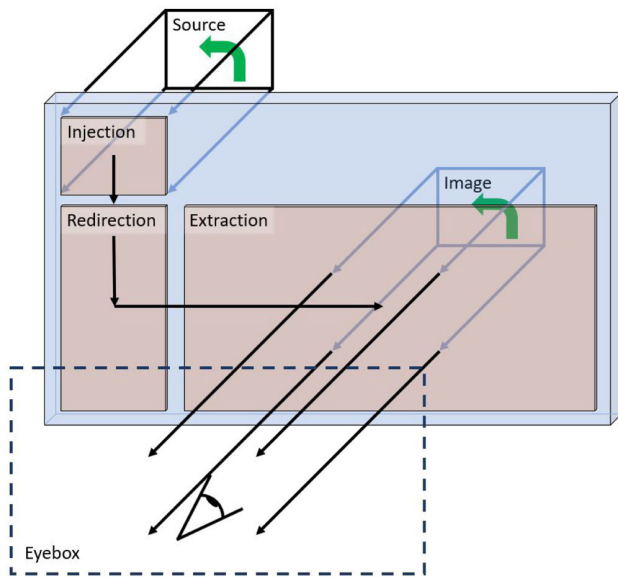


**Fig. 2.** Light from an outside source is projected through the waveguide HOE system to present an image to the observer over an expanded eyebox. Successive HOEs increase the exit pupil size, first vertically, then horizontally.

exit pupil is presented to the observer, which in turn allows the observer to see the unvignetted image farther from the waveguide surface. At viewing distances where an unexpanded exit pupil would present a clipped image to the observer, this system’s expanded exit pupil increases the observer’s experienced FOV. The diffraction efficiency (DE) of the redirection HOE is controlled to achieve uniform intensity across the entire beam profile as it propagates to the “extraction” [22]. The extraction HOE expands the eyebox horizontally using the same modulated DE technique and diffracts the light perpendicular to the waveguide surface, where it is visible to the observer.

The disadvantage of the L-shaped configuration shown in Fig. 2 is the spectral and angular selectivity of the redirection hologram, which limits the spectral bandwidth and range of

angles that can propagate through the entire system [23]. This selectivity may be useful for a system with monochromatic light and a narrow angular bandwidth, but wide-angle, white-light projectors are limited in what they can achieve with this design. Misalignment of the wavelength or incidence angle on the redirection hologram will reduce the intensity of diffracted light and steer the diffraction angle away from the lateral propagation necessary for the image to propagate to the extraction. This spectral and angular bandwidth is determined by the material properties of the redirection hologram and the hologram recording geometry. It can be overcome by multiplexing different gratings into the redirection hologram, but a different method can eliminate the need for such a heavily multiplexed hologram.

In this paper, a system is presented where a small injection hologram diffracts the incident light horizontally along the length of the waveguide to the extraction hologram. A surface relief grating (SRG) affixed to the waveguide surface along the propagation path causes vertical beam spreading, which yields an expanded FOV at the extraction. The SRG diffracts all visible wavelengths over a wide range of angles, avoiding the angular and spectral selectivity issues encountered with the L-shaped system. It also allows for a more compact system than the L-shaped design, which is helpful for space-constrained applications. A Zemax OpticStudio ray-tracing model was developed to demonstrate this design. Additionally, a physical system was built to support the concept. Both the model and the demonstrator achieved a FOV of  $16^\circ \times 14.25^\circ$ . Using the SRG, the vertical FOV was expanded from  $1.25^\circ$  to  $14.25^\circ$ .

The properties of the SRG allow it to perform its function of diffracting light over a wide angular and spectral bandwidth. The Thorlabs Reflective Holographic Grating with 1200 grooves/mm (50 mm  $\times$  50 mm) has an average DE of at least 30% from 250–1550 nm, which is more than enough to diffract all wavelengths from the pico-projector source. Additionally, the SRG is a thin grating and will diffract light from a wide range of incidence angles. This full-color, wide-angle diffraction is necessary to propagate an extended, white-light image through the system to the observer, which is something that was not possible

with the redirection hologram used in the L-shaped geometry. The current system design uses injection and extraction holograms that are sensitive only to 532 nm light, but future designs will seek to achieve a full-color display, using three-color multiplexed holograms.

## 2. METHODS

In this new in-line configuration, the incident, collimated light is diffracted along the length of the waveguide by the injection hologram. While light is reflecting within the waveguide due to TIR, interactions with the SRG expand the physical extent of the propagating beam. The extraction hologram diffracts the light perpendicular to the waveguide surface so that the projected image is visible to the user.

The internal propagation angle of the small injection hologram is chosen such that normally incident light is diffracted at the angle bisector of the critical angle and a maximum angle determined by the dimensions of the waveguide and the injection hologram. This angle is defined such that the left-most edge of the image that has reflected once within the waveguide is incident at the right edge of the injection hologram and is calculated according to

$$\theta_{\max} = \tan^{-1} \left( \frac{w/2}{t} \right), \quad (1)$$

with  $w$  the width of the injection hologram and  $t$  the thickness of the waveguide. Light diffracted beyond this maximum angle will lead to a discontinuous image where a stitching gap is visible between the different extraction regions. Figure 3 shows these angles.

The SRG diffracts the internally propagating light into +1, -1, and zero diffraction orders, which reflect within the waveguide due to TIR before they again interact with the SRG. At the second interaction, light that remained in the zero order is diffracted into its own +1, -1, and zero orders. Light in the  $\pm 1$  orders is either diffracted by the SRG back to the zero order propagation direction or continues in the direction of the first diffraction. It is the light that went from the  $\pm 1$  orders back into the zero order that expands the pupil vertically. Continued interaction with the SRG replicates the beams traveling in the +1, -1, and zero orders several times, much like a branching tree, which allows for a continuous expansion of the pupil. Figure 4 shows this branching pattern. Only light in the zero order diffraction direction is diffracted by the extraction hologram toward the observer. Light propagating in the  $\pm 1$  order diffraction directions is not outcoupled from the waveguide by

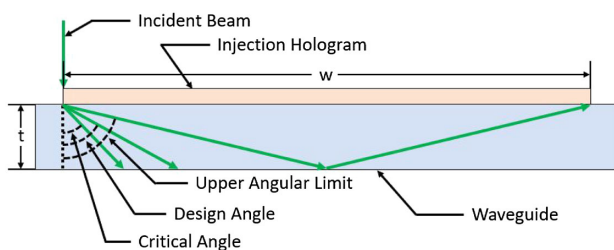


**Fig. 3.** Propagation angle is chosen to bisect the critical angle and the angle defined by Eq. (1).

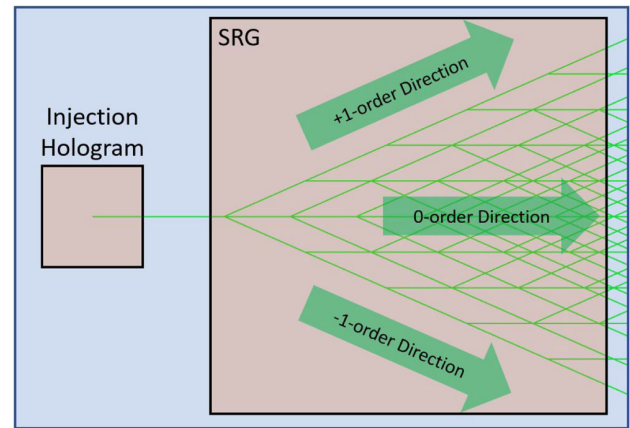


**Fig. 4.** Cross-sectional splitting of incident light by SRG. After the first interaction with the grating, light is diffracted into +1, -1, and zero diffraction orders. Light in the zero order is again split into the +1, -1, and zero orders, while light diffracted into the  $\pm 1$  orders is not diffracted or diffracted back to the zero order direction.

the extraction hologram. In fact, the image carried by the  $\pm 1$  order diffraction directions is flipped vertically and contains other aberrations. No information is lost by neglecting the  $\pm 1$  orders; this reduces only the intensity of the displayed image.

The extraction hologram was recorded to diffract a beam incident from inside the waveguide at the same angle determined by Eq. (1) to the hologram plane's surface normal. The extraction grating was also recorded with its DE modulated for low efficiency on the side of the grating nearest the injection hologram and the SRG and maximum efficiency on the far edge. This modulated DE was for uniform intensity of the image when viewed across the length of the extraction and was discussed in a previous publication [22]. The multiple interactions across the width of the extraction hologram causes horizontal pupil expansion.

## 3. COMPUTER MODELING

Modeling this system in Zemax OpticStudio's Non-Sequential mode demonstrated the feasibility of the design discussed in Section 2. The system was constructed with a design wavelength of 532 nm (350 nm used in the hologram lens recording parameters due to the wavelength reduction from the refractive index of the glass). The waveguide used in this model was a rectangular volume made of BK-7 glass (215 mm  $\times$  305 mm  $\times$  3.175 mm), while the injection and extraction holograms were hologram lens elements with dimensions of 12.7 mm  $\times$  12.7 mm  $\times$  16  $\mu$ m and 63.5 mm  $\times$  63.5 mm  $\times$  16  $\mu$ m, respectively. From Eq. (1), the maximum propagation angle for this design is 63.4°, and the critical angle for 532 nm light propagating through BK-7 glass is 41.8°. Thus, the injection hologram was designed to diffract collimated, normally incident 532 nm light at 52.6° within the waveguide. Because the light traveled within the waveguide at 52.6°, the extraction hologram was designed to diffract this light perpendicular to the hologram surface, toward the observer. The modulated DE of the grating was modeled by a series of eight glass plates with reflectivity increasing according to

$$R_i = \frac{1}{N_{\text{tot}} - N_i + 1}, \quad (2)$$

where  $R_i$  is the reflectivity of the  $i$ th glass plate,  $N_{\text{tot}}$  is the total number of segments (in this case, eight), and  $N_i$  is the number of the plate.

The SRG was modeled using the Lenslet Array 1 function in Zemax. The material was BK-7 glass, and dimensions were  $50 \text{ mm} \times 50 \text{ mm} \times 16 \text{ }\mu\text{m}$  with a grating spacing of 1200 lines/mm. This grating spacing was chosen because it gives a diffraction angle of  $24.8^\circ$ , which corresponds to a 46 mm vertical extent of the replicated zero order when propagated 50 mm across the length of the SRG. At a viewing distance of 150 mm, this 46 mm zero order will offer a maximum vertical FOV of  $17.5^\circ$  to the observer. The DE of the grating in the Lenslet Array 1 function was set under the Diffraction tab of the Object Properties menu so that 33% of the light was reflected into each of the +1, -1, and zero diffraction orders.

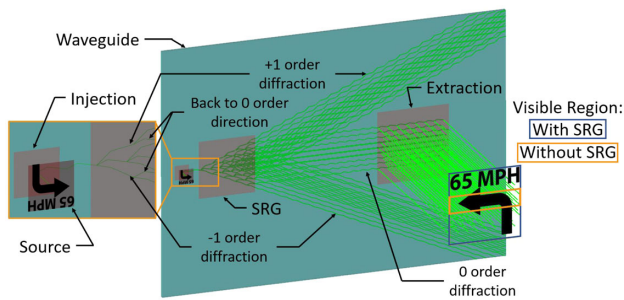


**Fig. 5.** Light incident from the source is diffracted at the design angle by the injection hologram. Light incident on the SRG is split into the +1, -1, and zero diffraction orders. Subsequent interactions with the SRG continue diffraction into one of the three propagation directions. The variable DE extraction hologram diffracts the expanded “zero order” toward the observer. The image inset provides an enlarged view of the branching diffraction that is caused by the SRG. Without the SRG, only a narrow portion of the image would be displayed.

To simulate the projection system, a collimated source was projected through an absorbing image filter. This collimated source object was imaged by a paraxial lens to locate the image at optical infinity. A 4 mm detector situated behind the extraction allowed for analysis of the system output as might be seen by the human eye. Figure 5 shows the completed OpticStudio design.

Light that remained in the +1 or -1 order diffraction direction did not contribute to the final image visible in the extraction. In this design, the light propagating in these directions remained within the waveguide before it was either out-coupled or scattered at the waveguide edges. The amount of light that is lost in these directions is determined by the DE and size of the SRG, as higher efficiency gratings diffract more light into the +1 and -1 orders, but subsequent interactions diffract the light in those non-zero orders back to the initial propagation direction. Figure 6 shows how the grating parameters of the SRG were optimized in this ray-tracing model. It was found that 33% diffraction into each of the +1, -1, and zero diffraction orders created the most uniform intensity distribution while maintaining image quality. At higher DE, image quality decreases, and at lower DE, the zero order is drastically brighter than the rest of the image. Similarly, the SRG was optimized so that, with physical dimensions of  $50 \text{ mm} \times 50 \text{ mm}$ , the full image was visible at the extraction.

#### 4. PHYSICAL DEMONSTRATOR

A physical demonstrator of this design configuration was created based on the parameters laid out in Section 3. The waveguide had dimensions of  $215 \text{ mm} \times 305 \text{ mm} \times 3.175 \text{ mm}$  and was made of a low-iron glass to decrease the absorption of light as it propagated inside the medium. The injection and extraction holograms were recorded with the same dimensions as in Section 3 using Bayfol HX200 photopolymer, a holographic recording film that is sensitive across the visible spectrum. Bayfol

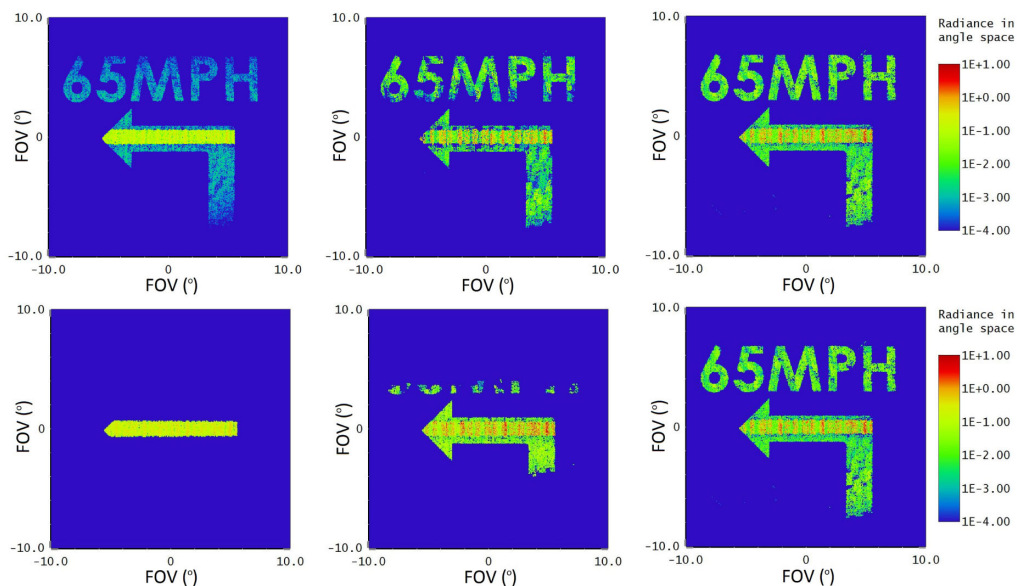


**Fig. 6.** (Top) 5%, 50%, and 33% DE to  $\pm 1$  diffraction orders. 33% DE maintains image quality without sacrificing uniform intensity. (Bottom) No SRG,  $25 \text{ mm} \times 25 \text{ mm}$  SRG, and  $50 \text{ mm} \times 50 \text{ mm}$  SRG. Increasing grating size allows for more of the projected image to be visible.

HX200 is easy to apply and cures with ultra-violet (UV) exposure. Additionally, the photopolymer is 16  $\mu\text{m}$  thick, allowing for a wide angular bandwidth of injected light.

The injection hologram was recorded to diffract a beam incident at the surface normal to  $52.6^\circ$ , and the extraction was recorded to diffract a beam incident at  $52.6^\circ$  to the hologram surface normal, just as in the computer model described in Section 3. The SRG is a Thorlabs reflective holographic grating (G50-12V) and was coupled to the waveguide using index-matching oil. A 3M MP220 incoherent, white-light mobile projector was set up so that the projector was flush with the injection hologram and focused as far away as possible to provide accommodation at infinity. In the demonstrator, the extraction was adjacent to the SRG, which kept all relevant optical components confined within a cube with side lengths of 200 mm. Figure 7 shows the demonstrator setup described here.

Figure 8 shows the physical demonstrator in operation with a projected image overlaid on a background scene. Figure 8(a) shows the scene visible when an observer focuses on the HUD itself: both the projected image and the background scene are out of focus. However, when the observer shifts his/her focus to the far field [Fig. 8(b)], both the background and the projected image come into focus. The FOV of this HUD demonstrator is  $16^\circ \times 14.25^\circ$ , which agrees with the results predicted by the computer model.

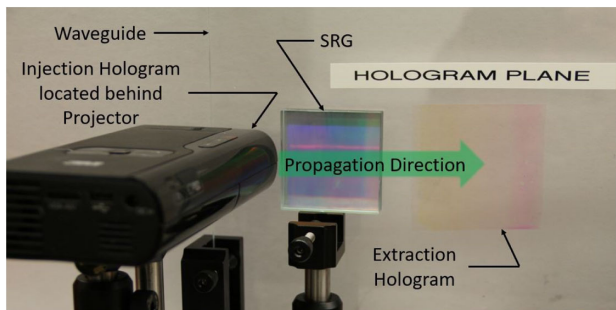


**Fig. 7.** Physical demonstrator of in-line pupil expansion HUD setup. Injection and extraction holograms are recorded in Bayfol HX200, which is attached to the waveguide surface. The SRG is coupled to the waveguide with index-matching fluid. The projector is pushed flush to the waveguide surface, minimizing the footprint of the system.

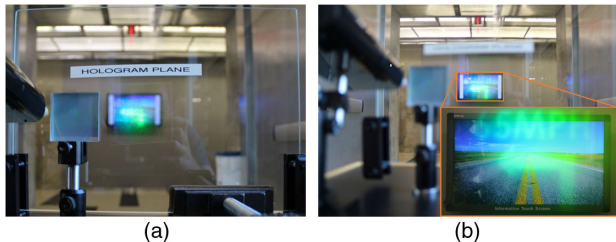


**Fig. 8.** Demonstrator shown in Fig. 7 is set up with an image projected in the background. When focusing on the waveguide plane, the image is not clear. Only when focus changes to the far field does the image become clear. Though the image visible in this scene is green, changing the observer's viewing position from left to right changes the color of the displayed image from violet to red. (a) Focused at the waveguide plane; (b) focused at optical infinity.

The image visible in Fig. 8(b) demonstrates some blur, which is visible both with and without the SRG attached and is thus due to scattering from repeated interactions with the injection and extraction holograms. Bayfol material has demonstrated this property in previous research efforts [22], but its ease of use continues to make it a valuable tool for exploratory holographic research.

## 5. CONCLUSION

This paper presented an HUD display system that used HOEs and an SRG affixed to a planar waveguide to achieve vertical and horizontal pupil expansion with an in-line geometry. This geometry has an advantage over the previously demonstrated L-shaped 2D pupil expansion because the SRG demonstrated  $33 \pm 5\%$  DE into the  $\pm 1$  diffraction orders from 450 nm–600 nm with unpolarized incident light [24] and an angular bandwidth of  $70^\circ$  according to the grating equation [25]. Both a Zemax OpticsStudio computer model and a physical demonstrator of the system were created that achieved pupil expansion and a FOV of  $16^\circ \times 14.25^\circ$ . The physical demonstrator could be fit into a 200 mm cube by removing unused portions of the waveguide, which demonstrates the compact nature of this system.

A future research direction for this technology would be to explore using different materials for the injection and extraction holograms. Using a holographic material with low scattering, such as dichromated gelatin (DCG), will improve the contrast and resolution of the display system. While a thicker hologram might reduce the acceptance angle, multiplexing several angles into one hologram would expand the angular acceptance of the injection and extraction gratings, supporting a larger system FOV or a full-color display.

Another area of future research would focus on having a fully holographic 3D HUD. As the injection and extraction HOEs and the SRG described in this research effort are static optical elements that relay light from the dynamically updating source to the observer, the image projector can be replaced with a holographic projector, such as a diffractive spatial light phase modulator (SLM), requiring only minor adjustments of the HOEs. Using a diffractive SLM instead of an imaging pico-projector would mean that the projected image would not necessarily be located at infinity, so the beam propagating within the waveguide would not be as well collimated. This might require altering the injection hologram, either by multiplexing it to accommodate different injection angles or by encoding it with some optical power.

Beyond HUD applications, this technology could also be applied to augmented reality glasses to achieve an expanded FOV with a small form factor.

**Funding.** National Science Foundation (1640329); University of Arizona.

**Acknowledgment.** The authors would like to thank Arkady Bablumyan for his insight. They would also like to acknowledge Laura Anderson and Sasaan Showghi for their help exploring SRG replication.

**Disclosures.** The authors declare that there are no conflicts of interest related to this paper.

## REFERENCES

1. Y.-C. Liu and M.-H. Wen, "Comparison of head-up display (HUD) vs. head-down display (HDD): driving performance of commercial vehicle operators in Taiwan," *Int. J. Hum.-Comput. Stud.* **61**, 679–697 (2004).
2. M. Ablaßmeier, T. Poitschke, F. Wallhoff, K. Bengler, and G. Rigoll, "Eye gaze studies comparing head-up and head-down displays in vehicles," in *IEEE International Conference on Multimedia and Expo* (2007), pp. 2250–2252.
3. C. Wickens and P. Ververs, "Allocation of attention with head-up displays," Tech. rep. (Aviation Research Laboratory, Institute of Aviation, 1998).
4. S. Fadden, C. D. Wickens, and P. Ververs, "Costs and benefits of head up displays: an attention perspective and a meta analysis," SAE Technical Paper 2000-01-5542 (SAE International, 2000).
5. W. J. Horrey, C. D. Wickens, and A. L. Alexander, "The effects of head-up display clutter and in-vehicle display separation on concurrent driving performance," *Proc. Hum. Factors Ergon. Soc. Annu. Meet.* **47**, 1880–1884 (2003).
6. J. Upatnieks, "Compact head-up display," U.S. patent 4, 711, 512 (8 December 1987).
7. R. B. Wood and M. J. Hayford, "Holographic and classical head up display technology for commercial and fighter aircraft," *Proc. SPIE* **0883**, 36–52 (1988).
8. H. Kato, H. Ito, J. Shima, M. Imaizumi, and H. Shibata, "Development of hologram head-up display," SAE Technical Paper 920600 (SAE International, 1992).
9. M. H. Kalmanash, "Digital HUDs for tactical aircraft," *Proc. SPIE* **6225**, 62250L (2006).
10. H. Peng, D. Cheng, J. Han, C. Xu, W. Song, L. Ha, J. Yang, Q. Hu, and Y. Wang, "Design and fabrication of a holographic head-up display with asymmetric field of view," *Appl. Opt.* **53**, H177–H185 (2014).
11. J. Han, J. Liu, X. Yao, and Y. Wang, "Portable waveguide display system with a large field of view by integrating freeform elements and volume holograms," *Opt. Express* **23**, 3534–3549 (2015).
12. P. Coni, S. Hourlier, A. Gueguen, X. Servantie, and L. Lалуque, "50-3: a full windshield head-up display using simulated collimation," *SID Symp. Digest Tech. Pap.* **47**, 684–687 (2016).
13. P. Coni, S. Hourlier, X. Servantie, L. Lалуque, and A. Gueguen, "A 3D head up display with simulated collimation," SAE Technical Paper 2016-01-1978 (SAE International, 2016).
14. C. H. Vallance, "The approach to optical system designs for aircraft head up displays," *Proc. SPIE* **0399**, 15–25 (1983).
15. C. T. Bartlett, M. L. Busbridge, and O. T. Horton, "Considerations of a head-up display field of view," *Proc. SPIE* **4712**, 468–479 (2002).
16. P. L. Wisely, "Head up and head mounted display performance improvements through advanced techniques in the manipulation of light," *Proc. SPIE* **7327**, 732706 (2009).
17. J. A. Cox, T. A. Fritz, and T. R. Werner, "Application and demonstration of diffractive optics for head-mounted displays," *Proc. SPIE* **2218**, 32–40 (1994).
18. A. A. Cameron, "Optical waveguide technology and its application in head-mounted displays," *Proc. SPIE* **8383**, 83830E (2012).
19. S. D. Harbour, "Three-dimensional system integration for HUD placement on a new tactical airlift platform: design eye point vs. HUD eye box with accommodation and perceptual implications," *Proc. SPIE* **8383**, 83830V (2012).
20. M. Homan, "The use of optical waveguides in head up display (HUD) applications," *Proc. SPIE* **8736**, 87360E (2013).
21. I. K. Wilmington and M. S. Valera, "Paper no 18.2: waveguide-based display technology," *SID Symp. Digest Tech. Pap.* **44**, 278–280 (2013).
22. C. M. Bigler, P.-A. Blanche, and K. Sarma, "Holographic waveguide heads-up display for longitudinal image magnification and pupil expansion," *Appl. Opt.* **57**, 2007–2013 (2018).
23. C. T. Draper, C. M. Bigler, M. S. Mann, K. Sarma, and P.-A. Blanche, "Holographic waveguide head-up display with 2-D pupil expansion and longitudinal image magnification," *Appl. Opt.* **58**, A251–A257 (2019).
24. "Reflective holographic gratings," 2019, [https://www.thorlabs.com/newgrouppage9.cfm?objectgroup\\_id=25](https://www.thorlabs.com/newgrouppage9.cfm?objectgroup_id=25).
25. P.-A. Blanche, *Field Guide to Holography* (SPIE, 2014).